A. J. Rosakis
Research Assistant.

L. B. Freund
Professor and Chairman.
Fellow ASME.

Division of Engineering,
Brown University,
Providence, R. I. 02912

The Effect of Crack-Tip Plasticity on the Determination of Dynamic Stress-Intensity Factors by the Optical Method of Caustics

The shadow spots which are obtained in using the optical method of caustics to experimentally determine dynamic stress-intensity factors are usually interpreted on the basis of a static elastic crack model. In this paper, an attempt is made to include both crack-tip plasticity and inertial effects in the analysis underlying the use of the method in reflection. For dynamic crack propagation in the two-dimensional tensile mode which is accompanied by a Dugdale-Barenblatt line plastic zone, the predicted caustic curves and corresponding initial curves are studied within the framework of plane stress and small scale yielding conditions. These curves are found to have geometrical features which are quite different from those for purely elastic crack growth. Estimates are made of the range of system parameters for which plasticity and inertia effects should be included in data analysis when using the method of caustics. For example, it is found that the error introduced through the neglect of plasticity effects in the analysis of data will be small as long as the distance from the crack tip to the initial curve ahead of the tip is more than about twice the plastic zone size. Also, it is found that the error introduced through the neglect of inertial effects will be small as long as the crack speed is less than about 20 percent of the longitudinal wave speed.

1 Introduction

Progress toward understanding the phenomenon of dynamic crack propagation in solids has been impeded by several complicating features which are encountered in both analytical and experimental approaches. From the experimental viewpoint, the inherent time dependence of the process requires that many sequential measurements of field quantities be made in an extremely short time in a way which does not interfere with the process itself. Furthermore, the place at which field quantities are to be measured varies, often in a nonuniform way, during the course of the process. Because of this complexity, most experimental techniques for measuring crack-tip stress and deformation fields during rapid fracture are based on optics. Such methods have three main advantages:

(*i*) The techniques are full-field methods, i.e., the entire specimen is observed continuously and crack paths need not be known *a priori.*

(*ii*) There is no coupling between the optical and mechanical processes, i.e., the method of measurement does not interfere with the process being examined.

(*iii*) The response of an optical system is essentially instantaneous on the time scale of mechanical rapid fracture events.

Several optical methods have been used during the past 50 years to measure deformations in nominally elastic materials, and thereby to determine stress fields. Most of the methods are based on light wave interference principles, and their application has been confined to transparent materials, or to opaque materials coated with transparent materials.

Recently, the optical method of caustics, or the shadow spot method, was developed and applied in the investigation of nonuniform surface deformations due to stress concentrations in deformed solids [1, 2]. Details of the stress field may then be inferred from shadow spot measurements on the basis of an analytical model. The method of caustics is an exceptional method because it is based on the principles of geometrical optics, rather than light interference, and it has been successfully applied to cases of both opaque and transparent materials. The method was first used in a reflection arrangement by Theocaris [2], who studied the stress singularity in the vicinity of a stationary crack tip. Later, Theocaris and Gdoutos [3, 4] applied the method of caustics in reflection to experimentally examine the de-
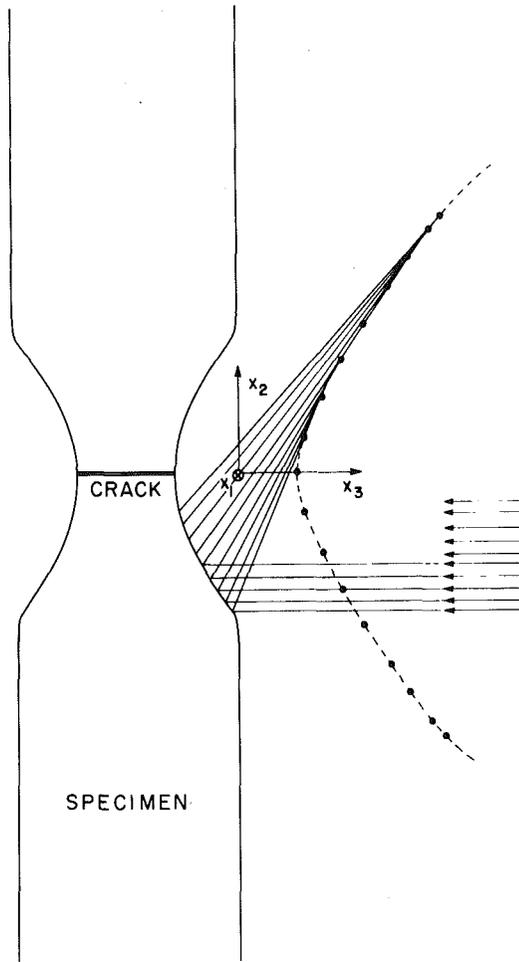
Fig. 1 Schematic of the formation of the three-dimensional caustic envelope obtained by reflection

$$f = -u_3 = \frac{\Delta s}{2} = \frac{\nu d}{2E}\left[(\sigma_{11}+\sigma_{22})\right]$$

Fig. 2 Optical mapping of points $P(x_1, x_2)$ of the surface of an illuminated solid, to points $P'(X_1, X_2)$ on a screen

formation fields near the tips of stationary cracks in metal plates. In this case, which apparently was the first application of the method to metal specimens, plastic deformation occurred locally and the optical data were analyzed by assuming a plane stress Dugdale-Barenblatt model for the crack-tip plastic zones.

The method was first used in experiments involving very rapid crack propagation and stress wave loading by Kalthoff and coworkers [5] and Theocaris and coworkers [6, 7], and more recently by Goldsmith [8]. In each case, it was assumed that the elastic stress field near the tip of a rapidly growing crack in a brittle solid has precisely the same spatial variation as the elastic stress field near the tip of a stationary crack. That is, the influence of inertial effects on the spatial dependence of the crack-tip field was not taken into account. More recently, several investigators have reanalyzed the method of caustics as applied to rapid crack propagation in brittle materials, including the effect of inertia on the spatial variation of the elastic crack-tip stress field. Kalthoff, et al. [9], introduced an approximate correction factor to account for the potentially large error introduced when the static local field is used in data analysis. The exact equations of the caustic envelope formed by the reflection of parallel incident light from the surface of a specimen containing a rapidly growing crack were recently obtained by Rosakis [10] for mixed mode plane-stress crack growth. It was found that, for some typical laboratory materials used in crack propagation studies, the neglect of the influence of inertia on the crack-tip stress field could lead to errors of up to 30 to 40 percent in the value of the elastic stress-intensity factor inferred from the measured caustic diameter. A similar analysis has also been discussed by Theocaris, et al. [11].
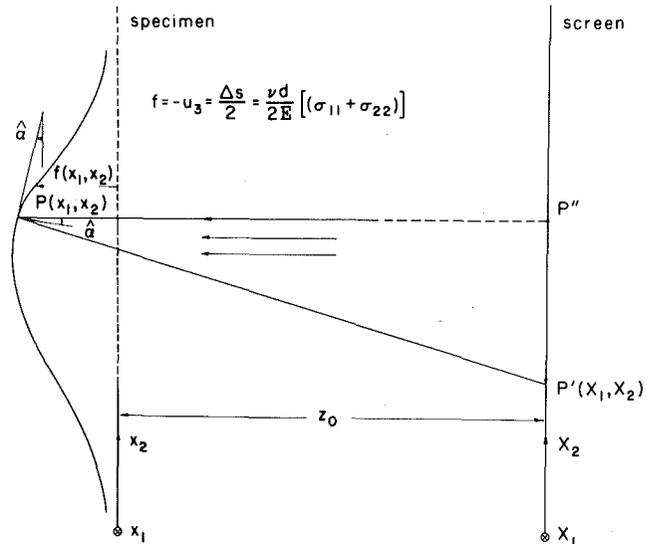
In this paper, a first attempt is made at including plasticity effects in the analysis underlying the optical method of caustics as applied in dynamic crack propagation studies. The analysis is based on the one-dimensional line plastic zone model of Dugdale and Barenblatt. For dynamic crack propagation in the two-dimensional tensile mode which is accompanied by such a strip yield zone, the sizes and shapes of the predicted caustic curves are studied. The influence of material inertia and of the extent of the plastic zone on stress-intensity factor measurements are considered. The initial and caustic curves are found to have geometrical features quite different from those present for purely elastic crack growth, and the dependence of these features on crack speed and plastic zone size is investigated.

2 Formation of Caustics in Reflection

Consider a family of parallel light rays incident on the reflective surface $x_3 = -f(x_1, x_2)$ of an opaque material; see Fig. 1. Upon reflection from the surface, the light rays will deviate from parallelism. (In practice, the intensity of the reflected ray will be less than the intensity of the incident ray due to random scattering.) If certain geometrical conditions are met by the reflecting surface, then the family of reflected rays will have an envelope in the form of a three-dimensional surface in space. A section of such a surface is shown as the dashed curve in Fig. 1. This surface, which is called the *caustic surface*, is the locus of points of maximum luminosity (i.e., highest density of rays) in the reflected field. The reflected rays are tangent to the caustic surface. If a screen is positioned parallel to the (x_1, x_2)-plane and so that it intersects the caustic surface, then a cross section of the caustic surface can be observed as a bright curve (the so-called *caustic curve*) bordering a relatively dark region (the *shadow spot*) on the screen.

Suppose that the incident ray which is reflected from the point $P(x_1, x_2)$ on the reflecting surface will intersect the screen at the image point $P'(X_1, X_2)$; see Fig. 2. The (X_1, X_2) coordinate system is identical to the (x_1, x_2) system, except that the origin of the former has been translated to the screen. The position of the image point P' will depend on the slope of the reflecting surface at P and on the normal distance z_0 between the screen and the reflecting surface. It has been shown elsewhere [12] that the position of the image point P' on the screen has coordinates

$$X_i = x_i \pm 2z_0(\partial f/\partial x_i) \tag{1}$$

where $z_0 \gg |f|$. Equation (1) represents a mapping of points P of the reflecting surface onto points P' of the screen. The choice of sign in

(1) depends on whether the image point is a real image in front of the reflecting surface (+ sign) as is the case in Fig. 2 or a virtual image behind the reflecting surface (− sign). The use of the virtual image has certain advantages in experimental fracture mechanics, and the subsequent analysis will be based on the choice of the negative sign in (1).

If the screen intersects a caustic surface, then the resulting caustic curve on the screen is a locus of points of multiple reflection. That is, for those points on the caustic curve, the mapping (1) is not invertible and the Jacobian of the transformation must vanish, i.e.,

$$J(x_1, x_2) = \frac{\partial(X_1, X_2)}{\partial(x_1, x_2)} = 0 \qquad (2)$$

The vanishing of the Jacobian is the necessary and sufficient condition for the existence of a caustic curve. The points on the reflecting surface for which $J(x_1, x_2) = 0$ are the points from which the rays forming the caustic curve are reflected. The locus of these points on the reflecting surface is the so-called *initial curve*.

3 Application of Caustics to Plane-Stress Elastodynamics

Consider a two-dimensional elastic solid occupying a region of the x_1, x_2-plane. The outer boundary is subjected to traction and/or displacement boundary conditions of a type to ensure uniqueness of solution. Suppose that a planar crack grows through the body, with the crack tip speed being v. Within the framework of the theory of plane stress, the two-dimensional displacement vector $\mathbf{u}$ is governed by the equation

$$c_l^2 \nabla(\nabla \cdot \mathbf{u}) - c_s^2 \nabla \times \nabla \times \mathbf{u} = \ddot{\mathbf{u}} \qquad (3)$$

where ∇ is the two-dimensional gradient operator and the superposed dot denotes time derivative. In terms of the elastic modulus E and Poisson's ratio ν, the longitudinal and shear wave speeds for plane stress are $c_l = [E/(1 - \nu^2)\rho]^{1/2}$ and $c_s = [E/2(1 + \nu)\rho]^{1/2}$, respectively.

Any displacement vector which is derived from the longitudinal and shear wave potentials ϕ and ψ according to

$$\mathbf{u} = \nabla\phi + \nabla \times \boldsymbol{\psi}; \quad c_l^2 \nabla^2 \phi - \ddot{\phi} = 0; \quad c_s^2 \nabla^2 \boldsymbol{\psi} - \ddot{\boldsymbol{\psi}} = 0 \qquad (4)$$

satisfies (3). In plane stress, $\boldsymbol{\psi}$ has a single nonzero component which is here denoted by ψ.

Suppose now that the (x_1, x_2) coordinate system is fixed with its origin at the moving crack tip and that it is oriented so that crack growth is in the x_1-direction. Furthermore, suppose that the crack grows with constant speed, and that the geometry and applied loading are steady (i.e., independent of time) as seen by an observer moving with the crack tip. Under these circumstances, it is expected that the complete elastodynamic field is steady, so that ϕ and ψ depend only on x_1, x_2 and (˙) = $-v\partial(\ )/\partial x_1$. Under steady conditions, the wave equations in (4) reduce to

$$\frac{\partial^2 \phi}{\partial x_1^2}\left(1 - \frac{v^2}{c_l^2}\right) + \frac{\partial^2 \phi}{\partial x_2^2} = 0 \qquad \frac{\partial^2 \psi}{\partial x_1^2}\left(1 - \frac{v^2}{c_s^2}\right) + \frac{\partial^2 \psi}{\partial x_2^2} = 0 \qquad (5)$$

But each of the reduced wave equations is clearly equivalent to Laplace's equation with the x_2 coordinates scaled by the factor $\alpha_l = (1 - v^2/c_l^2)^{1/2}$ in the first case and $\alpha_s = (1 - v^2/c_s^2)^{1/2}$ in the second case. General solutions of (5) may be written immediately in the form

$$\phi = \text{Re}\,[F(z_l)], \quad \psi = \text{Im}\,[G(z_s)] \qquad (6)$$

where $z_l = x_1 + i\alpha_l x_2$, $z_s = x_1 + i\alpha_s x_2$, and F and G are each an analytic function of its complex argument in the region occupied by the body. In any given problem, the analytic functions are determined by the boundary conditions. Although (5)–(6) have been established with reference to crack growth, it should be noted that these equations are valid for any steady plane-stress elastodynamic field.

Generally, for plane-stress crack propagation in a body which is symmetric about the crack plane, the deformation fields are a combination of two modes. The tensile mode, or Mode I, exhibits reflective symmetry with respect to the crack plane, while the shearing mode,

or Mode II, is antisymmetric with respect to the crack plane. For these cases

$$F(\bar{z}_l) = \pm \overline{F(z_l)}, \quad G(\bar{z}_s) = \pm \overline{G(z_s)} \qquad (7)$$

where the upper signs apply for Mode I and the lower signs for Mode II. The bar denotes complex conjugate.

Consider now a plate which has uniform thickness d in the undeformed state. If the plate is subjected to edge loading which results in a nonuniform state of plane stress, then the thickness of the deformed plate is also nonuniform. In terms of the in-plane stress components the lateral contraction is

$$f(x_1, x_2) = -u_3(x_1, x_2) = \nu d(\sigma_{11} + \sigma_{22})/2E \qquad (8)$$

Clearly, the function f here is identified with the function f describing the reflecting surface in Section 2. It represents the shape of the originally plane surface which is the reflecting surface.

In terms of the stress distribution, the equations of the mapping (1) based on geometrical optics become

$$X_i = x_i - C\partial(\sigma_{11} + \sigma_{22})/\partial x_i \qquad (9)$$

where $C = z_0 \nu d/E$. Thus determination of the first invariant of stress establishes the mapping, even for dynamic problems.

In terms of the displacement potential ϕ, the first stress invariant is

$$\sigma_{11} + \sigma_{22} = \frac{E}{(1 - \nu)} \nabla^2 \phi \qquad (10)$$

For a steady-state deformation field translating in the x_1-direction with speed v, (5) may be employed to reduce (10) to

$$\sigma_{11} + \sigma_{22} = (1 + \nu)\rho v^2 \partial^2 \phi/\partial x_1^2 \qquad (11)$$

or, in terms of the analytic function F appearing in the general solution (6),

$$\sigma_{11} + \sigma_{22} = (1 + \nu)\rho v^2 \,\text{Re}\,[F''(z_l)] \qquad (12)$$

If the differentiation indicated in (9) is performed and the result is expressed in terms of the complex variables $Z = X_1 + iX_2$, $z = x_1 + ix_2$ then the mapping is

$$Z = z - \kappa \{\text{Re}\,[F'''(z_l)] - i\alpha_l \,\text{Im}\,[F'''(z_l)]\} \qquad (13)$$

where $\kappa = (1 + \nu)\,\rho v^2 C$.

As noted in the preceding section, the condition for the existence of a caustic curve on the screen at $x_3 = -z_0$ is the vanishing of the Jacobian of the transformation (13). With reference to (2), the condition $J(x_1, x_2) = 0$ specifies the initial curve on the plane of the specimen, and the corresponding caustic curve on the screen is the map of the initial curve according to (13) onto the place of the screen. The condition that the determinant of the Jacobian matrix must vanish is

$$J = 1 + \kappa(1 - \alpha_l^2)\,\text{Re}\,[F^4(z_l)] - \alpha_l^2 \kappa^2 |F^4(z_l)|^2 = 0 \qquad (14)$$

where F^4 is the fourth derivative of F with respect to its argument.

The equations (13) and (14) together describe the caustic curves formed by reflection of parallel light from the surface of *any* planar elastic solid in which the elastodynamic stress distribution is steady. For any particular case, the analytic function F which appears in these equations must be determined from the geometrical configuration of the body and the boundary conditions.

In the case of elastic crack propagation, the stress field has universal spatial dependence in the vicinity of the crack tip. The only quantity which varies from one specific case to another is a scalar amplitude, the so-called elastic stress-intensity factor, which is often the parameter of fundamental interest in laboratory testing. In the context of equations (13) and (14), the function F will be known up to a scalar multiplier, the stress-intensity factor. If the crack speed, geometrical parameters, and bulk material parameters are known, the equations (13) and (14) then provide a relationship between a characteristic dimension of the caustic curve and the corresponding value of the

stress-intensity factor. Experimental measurement of this characteristic dimension provides the instantaneous value of the stress-intensity factor. The tremendous appeal of the method is due to the fact that it povides a *direct* measure of the stress-intensity factor in nominally elastic fracture. No measurement of boundary conditions or field quantities is required. The optical singularity on the screen provides the information necessary to determine the strength of the mechanical singularity in the specimen (under the assumption that the theory of plane stress provides an accurate picture of the three-dimensional deformation field).

4 Caustic Curves for the Line Plastic Zone Model

Analytical crack-tip models of a one-dimensional zone of nonlinear material response extending ahead of the tip have been proposed for plane-stress fracture of ductile sheets by Dugdale [13] and for the case of pure cleavage tensile fracture by Barenblatt, et al. [14]. The Dugdale-Barenblatt model is analyzed as an elastic crack problem in which the crack is made effectively longer by an amount R, the plastic zone size, with cohesive forces in the plastic zone acting on the prospective crack surfaces so as to restrain the opening. If small scale yielding conditions prevail then the applied loading is completely specified by an equivalent elastic stress-intensity factor, which is denoted by K_I for the plane tensile fracture model.

The analysis of the strip yield model is outlined in [15]. The (x_1, x_2) coordinate system is fixed at the tip which is moving with constant speed v in the x_1-direction. The plastic zone extends over the interval $0 < x_1 < R$. The derivation of the analytic function F, which is required to determine the caustic curves, follows closely the work of Willis [16] and employs the asymptotic result of Freund and Clifton [17]. For the case of small scale yielding and ideal plasticity, in which the cohesive tractions which resist crack opening in the plastic zone have the constant magnitude σ_0, the analytic function F is given by

$$F''(z) = \frac{2\sigma_0(1 + \alpha_s^2)}{\mu \pi Q} \tan^{-1} \left[\frac{R}{z - R} \right]^{1/2} \quad (15)$$

where

$$R = \frac{\pi K_I^2}{8\sigma_0^2}, \quad Q = 4\alpha_l \alpha_s - (1 + \alpha_s^2)^2 \quad (16)$$

The quantity σ_0 is identified as the uniaxial tensile flow stress of the material. The branch of $(z - R)^{1/2}$ which is positive as $z \to \infty$ along the positive real axis of the z-plane is assumed. Note that the relationship (16) between the plastic zone size and the remote stress-intensity factor is identical to the corresponding result for quasi-static deformations [18]. However, the function F is different from the corresponding quasi-static result.

Suppose now that a tensile crack is propagating in a polished plate specimen, and that the specimen is illuminated by a beam of parallel light as indicated in Fig. 1. The light will be reflected from the specimen surface and, under suitable conditions, will form a caustic curve on a screen placed at a distance z_0 from the midsurface of the specimen. The size and shape of the caustic curve will be related to the functional form of F in (15), and will depend on the parameters v, σ_0, and K_I. In what follows, the nature of the caustic curves corresponding to dynamic crack growth accompanied by a strip yield plastic zone under small scale yielding conditions is investigated. The investigation is based on the analytic function F given in (15) and (16), on the equation of the initial curve (14), and on the equation of the optical mapping (13).

Next, all lengths are normalized with respect to the plastic zone size R, and a superposed caret is used to denote normalized values of the length parameters, e.g., $\hat{z}_l = z_l/R = \hat{r}_l \exp(i\theta_l)$. If F is differentiated and is substituted into the equation for the initial curve (14), then the result in nondimensional form is

$$J(\hat{r}_l, \theta_l) = 1 - A(1 - \alpha_l^2) \operatorname{Re} [G(\hat{z}_l)] - \alpha_l^2 A^2 |[G(\hat{z}_l)]|^2 = 0 \quad (17)$$

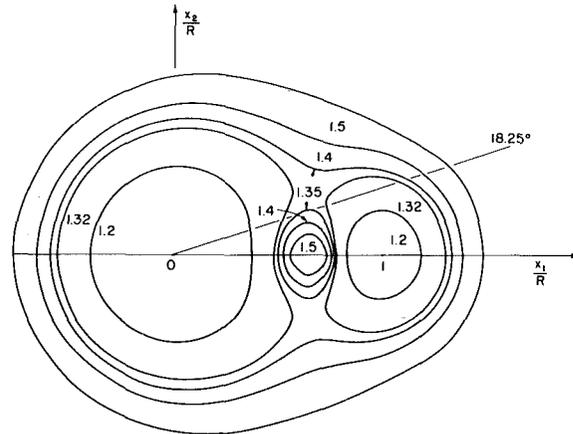where J is now viewed as a function of the distorted polar coordinates. In (17)

Fig. 3 Initial curves at the tips of steadily propagating cracks for five values of r/R

$$G(z) = \frac{(3z/2 - 1)}{z^2(z - 1)^{3/2}} \qquad A = \frac{(1 + \nu)\rho v^2(1 + \alpha_s^2)}{\pi Q} \frac{\sigma_0 z_0 \nu d}{ER^2} \quad (18)$$

The mapping, which defines the caustic curves corresponding to the solution of (17), is

$$\hat{X}_1 = \hat{r}_l \cos \theta_l + \frac{A}{\hat{r}_l(\hat{r}_l^2 - 2\hat{r}_l \cos \theta_l + 1)^{1/4}}$$
$$\times \cos \left[\theta_l + \frac{1}{2} \tan^{-1} \left(\frac{\hat{r}_l \sin \theta_l}{\hat{r}_l \cos \theta_l - 1} \right) \right] \quad (19a)$$

$$\alpha_l \hat{X}_2 = \hat{r}_l \sin \theta_l + \frac{\alpha_l^2 A}{\hat{r}_l(\hat{r}_l^2 - 2\hat{r}_l \cos \theta_l + 1)^{1/4}}$$
$$\times \sin \left[\theta_l + \frac{1}{2} \tan^{-1} \left(\frac{\hat{r}_l \sin \theta_l}{\hat{r}_l \cos \theta_l - 1} \right) \right] \quad (19b)$$

The limiting behavior of the foregoing equations as $R \to 0$ and $v \to 0$ may be checked against the previously derived results for $R = 0$ and $v = 0$. It is easily shown that if $R \to 0$ then (19) reduce to the equations (2.9) of [10] which represent the caustic envelope for a dynamic Mode I crack propagating in a linear elastic solid. For $R \to 0$ and $v \to 0$, (19) reduce to the equation of a generalized epicycloid as predicted by the analysis of a stationary crack in a linear elastic material [2].

5 Results and Discussion

Two parameters which seem to have fundamental significance in analyzing the initial curves (17) and caustic curves (19) are the ratio of crack-tip speed to characteristic speed of the material and the ratio of initial curve "size" to plastic zone size. The former parameter represents a measure of the inertial effects, while the latter parameter represents a measure of the influence of the crack-tip plastic zone. Furthermore, the two parameters are independent of each other, in the sense that either may be varied without influencing the other. Specifically, the *inertial parameter* is v/c_l and the *plasticity parameter* is r/R, which is understood to be the solution of (17) for $\theta_l = 0$. Thus r/R is the quotient of the distance from the crack tip to the extremity of the initial curve directly ahead of the crack tip and the length of the plastic zone R.

The equation of the initial curve (17) was solved numerically by means of the Newton-Raphson procedure. First, the value of θ_l was fixed, and then all values of $\hat{r}_l$ satisfying the resulting equation were determined by Newton-Raphson iteration. This was done for a number of values of θ_l sufficient to generate the initial curves.

The computed initial curves for the case of $v/c_l = 0.2$ are shown in Fig. 3 for a range of values of r/R. The geometrical features of the initial curves are strikingly different from the features of an initial curve for an elastic crack. For values of r/R near to unity (e.g., $r/R =$
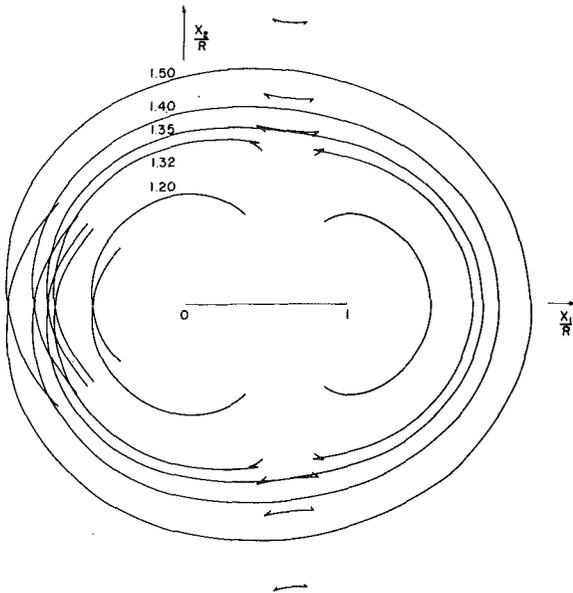
Fig. 4 Caustic curves formed by reflection from the near tip region of steadily propagating cracks corresponding to the initial curves of Fig. 3

Fig. 5 A detailed view of the cusped portion of the caustic curve for $r/R = 1.35$, $v = 0.20 \, c_l$, shown in Fig. 4

Fig. 6 Variation of the dimensionless maximum transverse diameter of the caustic curve, versus the normalized remote elastic stress-intensity factor, presented for a range of crack velocities

1.2), the individual singularities in the deformation field at the crack tip and the plastic zone tip dominate. The initial curve consists of two disjoint lobes, each roughly circular and centered at these two singularities. As r/R becomes larger, the shape of two lobes is distorted and they tend to approach each other. As seen in Fig. 3, the two lobes are almost in contact for $r/R = 1.32$. When r/R has increased to about 1.34, the two lobes have two common points. As r/R increases beyond this critical value (e.g., to $r/R = 1.35$), the initial curve again splits into two lobes. However, whereas the lobes are disjoint for $r/R < 1.34$, they are nested for $r/R > 1.34$. This nested structure is maintained as r/R is increased. For values of r/R large compared to one, the shape of the outer lobe is essentially the correct shape for a dynamic elastic crack. The inner lobe becomes very small compared to R as r/R becomes large, and is finally reduced to a point as $r/R \rightarrow \infty$.

It is a simple matter to prove that the initial curve (17) intersects the plastic zone at two points for *any* value of r/R in the range $1 < r/R < \infty$. On $\text{Im} \, (\hat{z}_l) = 0$ and $0 < \text{Re} \, (\hat{z}_l) < 1$, it is clear from (18) that $\text{Re} \, (G) = 0$, and (17) takes on the simple form

$$(\alpha_l A)^{-2} = |G(\hat{z}_l)|^2 \qquad (20)$$

The left side of (20) is, in general, a bounded positive real number. From (18), it can be seen that the right side of (20) equals zero if $\text{Re} \, (\hat{z}_l) = \frac{2}{3}$. Furthermore, the right side of (20) increases monotonically from zero to arbitrarily large values *either* as $\text{Re} \, (\hat{z}_l)$ increases from $\frac{2}{3}$ to 1 *or* as $\text{Re} \, (\hat{z}_l)$ decreases from $\frac{2}{3}$ to 0. Thus (20) always has one, and only one, root in the range $0 < \text{Re} \, (\hat{z}_l) < \frac{2}{3}$, and one, and only one, root in the range $\frac{2}{3} < \text{Re} \, (\hat{z}_l) < 1$. As $r/R \rightarrow \infty$, these two roots coalesce at $\hat{z}_l = \frac{2}{3}$. The coalescence of the two roots as $r/R \rightarrow \infty$ corresponds to the reduction of the inner loop of the initial curve to a single point as the effects of plasticity disappear.

The caustic curves corresponding to the initial curves in Fig. 3 are shown in Fig. 4. If the initial curve consists of disjoint lobes, then the resulting caustic consists of open curves (e.g., $r/R = 1.2$ in Fig. 4). As r/R approaches the transition value of 1.34, cusps are formed near the ends of the open curves. When r/R reaches the critical value of 1.34, the gap between the open curves which form the caustic closes, and as r/R increases beyond the critical value (e.g., for $r/R = 1.35$), the cusped portion of the curve splits off from the main caustic curve. A detailed view of these cusps for $r/R = 1.35$ is shown in Fig. 5, where the corresponding angle on the initial curve is identified for several points on the caustic. Note that the ends of the caustic seem to correspond to the points where the initial curve intersects the plastic
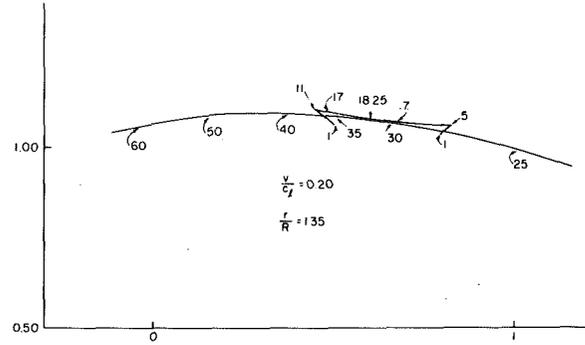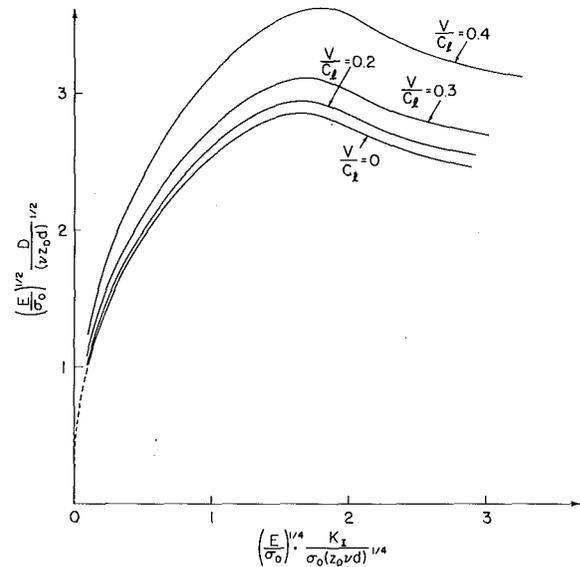
zone. For $r/R \geq 1.34$, the cusped segment of the caustic arises from the small inner loop of the initial curve, and the larger smooth portion of the caustic arises from the outer loop of the initial curve. As r/R increases, the small cusped segment of the caustic curve becomes smaller and separates further from the main part of the caustic curve.

6 Interpretation of Experiments

The following discussion is based on the assumption that, in the interpretation of experimental data, the size of the caustic curve is determined by the distance between the two points on the curve which are furthest from the X_1-axis on the screen. This distance will be denoted by D. For a purely elastic Mode I crack under quasi-static conditions, the relationship

$$\left[\left(\frac{E}{\sigma_0 \nu z_0 d} \right)^{1/2} D \right] = 2.5928 \left[\left(\frac{E}{\sigma_0 \nu z_0 d} \right)^{1/4} \frac{K_I}{\sigma_0} \right]^{2/5} \qquad (21)$$

between D and the Mode I stress-intensity factor K_I is well known. Although the plastic flow stress σ_0 appears in (21), it does so only through a factor common to both sides of the equation. The form of (21) was chosen because the results with plasticity effects included could be expressed best in terms of the dimensionless quantities in square brackets in (21).

For a given crack-tip speed v/c_l, both of the dimensionless quantities $D(E/\sigma_0 \nu \, z_0 d)^{1/2}$ and $(K_I/\sigma_0)(E/\sigma_0 \, \nu \, z_0 d)^{1/4}$ can be determined
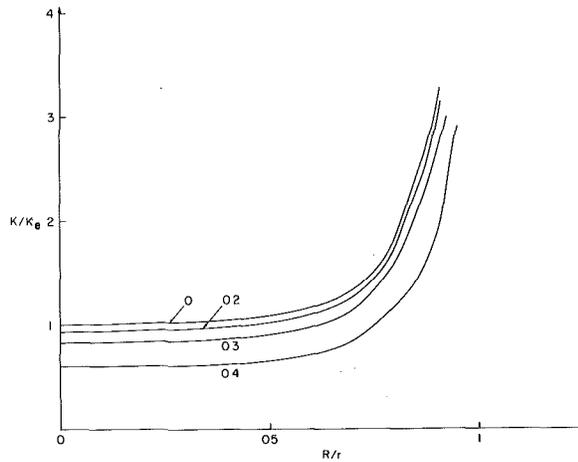
Fig. 7 Error introduced in the inferred value of K through neglect of both material inertia and plasticity effects in the analysis of experimental data

Fig. 8 Caustic formed in reflection at the tip of a propagating crack in a metallic specimen using single phase, monochromatic light

in terms of the parameter r/R, which is thus a parametric representation of the D versus K_{I} relationship. If the parameter r/R is eliminated (a process which can only be done numerically), then the relationship shown in Fig. 6 for four crack speeds is established. It is important to note that r/R varies alone each curve in Fig. 6, in general decreasing from left to right. The dashed curve in Fig. 6 is simply a graph of (21) which is valid for $v/c_l = 0$ and $r/R \rightarrow \infty$. As can be seen, it fits very well with the computed result for $v/c_l = 0$. It should perhaps be restated here that D is assumed to be the observed caustic size, K_{I} is the remote elastic stress-intensity factor within small scale yielding theory, and the relationship shown in Fig. 6 is that predicted on the basis of plane-stress theory, small scale yielding, and the Dugdale-Barenblatt one-dimensional plastic zone model. It would appear from Fig. 6 that if experimental observations are confined to cases for which $(K_{\mathrm{I}}/\sigma_0)(E/\sigma_0 \nu z_0 d)^{1/4}$ is less than about 1.0, then plasticity effects need not be taken into account in the interpretation of the observations. The possibility of adjusting the value of this nondimensional parameter simply by changing z_0 is only apparent because the value of this distance is not completely arbitrary. In any experimental setup for measuring stress-intensity factors by the method of caustics, the distance z_0 must be chosen so that the initial curve lies in a region of the specimen near the crack tip where the K-dominated small scale yielding solution accurately represents the stress field. It is also observed that the influence of inertia on the D versus K_{I} relationship is not large if v/c_l is less than about 0.2.

Suppose now that an observed caustic of size D is interpreted in two ways. First, it is interpreted on the basis of an elastic crack model and quasi-static conditions, and the inferred value of Mode I stress-intensity factor is K_e. Alternatively, the caustic is interpreted on the basis of a dynamic line plastic zone model, and the inferred value of the Mode I stress-intensity factor in this case is simply K. The ratio K/K_e as a function of r/R is shown in Fig. 7. This result suggests that, as long as the extent of the initial curve ahead of the crack tip is at least about twice the plastic zone size, the error introduced through neglect of plasticity effects in the analysis of the data will be small. Again, this observation is based on the condition that the initial curve lies in a region of the specimen in which the K-dominated small scale yielding solution accurately represents the stress field. A qualitative discussion of this oint is included in [19]. For any extent of the plastic zone, inertial effects seem to be important only for crack speeds in excess of $0.2\ c_l$.

Finally, two photographs of caustic curves obtained in reflection for running fractures in steel specimens are shown in Figs. 8 and 9. These are preliminary photographs taken in the process of developing an experimental apparatus, and a full quantitative interpretation is not yet available. However, it does seem that the caustics are elongated in the direction of crack growth, rather than circular as they would
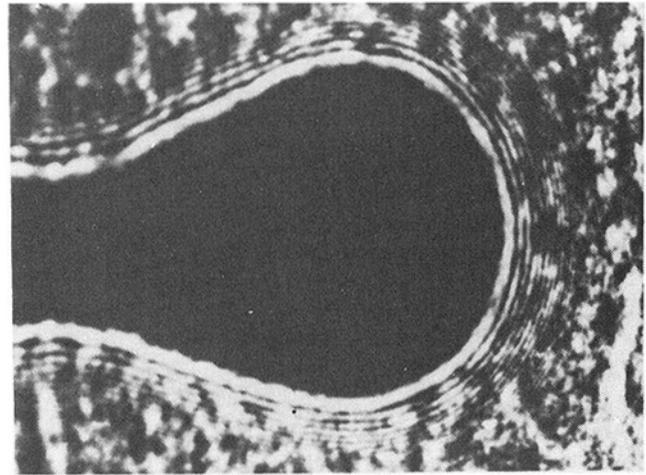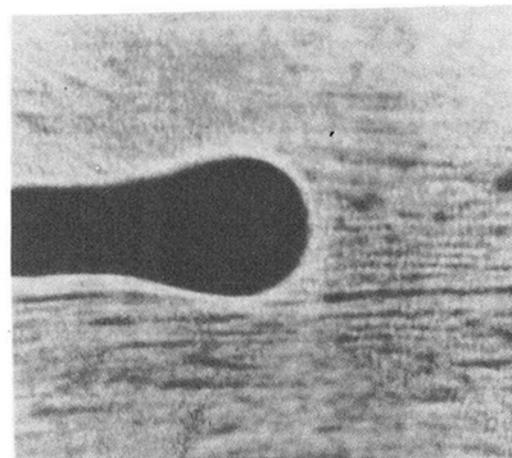

Fig. 9 Caustic formed in reflection at the tip of a propagating crack in a metallic specimen using white light
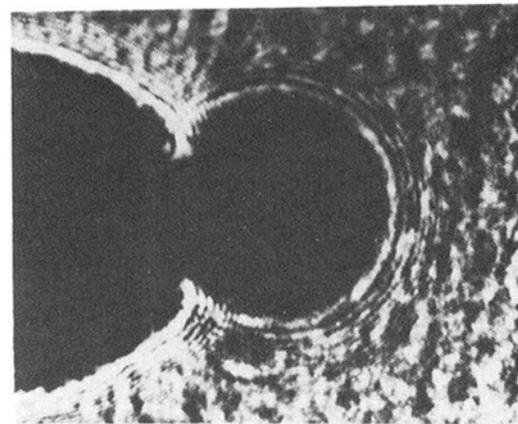

Fig. 10 Caustic at a stationary crack tip in the form of an epicycloid as predicted by elastic static analysis

be for an elastic crack as in Fig. 10. The long tail behind the main caustic curves is apparently due to the permanently deformed wake left behind as the active plastic zone passes by a material point. The Dugdale-Barenblatt crack-tip plastic zone model does not include a plastic wake effect, and no quantitative estimate of the relative size of the caustic associated with the wake region is yet available. The fringes in the optical pattern of Figs. 8 and 10 seem to be due to phase

interference. The light source used to produce the photographs shown in Figs. 8 and 10 was a laser which emits monochromatic, single phase light. The illumination outside the caustic curve results from a double reflection or mapping. That is, light waves reflected from both inside and outside the initial curve on the specimen strike the screen outside the caustic. Because of the deformation of the specimen surface, however, the light rays reflected from inside the initial curve travel a distance different from that traveled by the rays reflected from outside the initial curve. This difference in path length leads to a difference in phase at the screen which results in the observed phase interference pattern. Unlike Figs. 8 and 10, no fringes appear in the photograph in Fig. 9 because the incident light in this case was not single phase and no regular phase interference pattern could be formed.

7 Summary of Conclusions

For the line plastic zone model, the geometrical features of the initial and caustic curves are found to be strikingly different from the curves corresponding to an elastic crack. In terms of the fundamental parameters r/R and v/c, which were defined at the beginning of Section 5, the following observations are made:

1 With reference to the initial curve for $v/c = 0.2$,

(i) For r/R near unit, two disjoint lobes centered at $x_1 = 0$ and $x_1 = R$ are found.

(ii) As r/R increases from 1 to 1.34, the two lobes distort and approach each other.

(iii) The two lobes make contact when $r/R = 1.34$ and as r/R increases beyond 1.34, the initial curve takes the form of two nested closed curves.

(iv) As $r/R \to \infty$, the outer branch of the initial curve approaches the shape appropriate for a dynamic elastic crack and the inner branch shrinks to a single point on the line plastic zone.

2 With reference to the caustic curve for $v/c_l = 0.2$,

(i) For $1 < r/R < 1.34$, the caustic consists of two open curves.

(ii) As r/R increases toward 1.34, cusps are formed at the ends of the open curves and the separation distance between the two open curves decreases. The separation distance vanishes when $r/R = 1.34$.

(iii) For $r/R > 1.34$, the main part of the caustic is an oval curve with its longer axis in the direction of crack growth. A small secondary caustic, arising from the inner loop of the nested initial curve, splits off from the main caustic.

(iv) As $r/R \to \infty$, the main part of the caustic approaches the shape appropriate for a dynamic elastic crack and the secondary caustic vanishes.

3 On the basis of the line plastic zone model, plasticity effects need not be taken into account in analyzing experimental data for which $(E/\sigma_0 v z_0 d)^{1/4} (K_I/\sigma_0)$ is less than about 1.0.

4 The error introduced through the neglect of plasticity effects in the analysis of data will be small as long as the extent of the initial curve ahead of the crack tip is more than twice the plastic zone size.

5 Inertial effects appear to be significant for crack speeds exceeding approximately 0.2 c_l.

References

1 Manogg, P., "Anwendung der Schattenoptik zur Untersuchung des Zerreisvorganges von Platten," Dissertationsschrift an der Universität Freiburg, 1964.

2 Theocaris, P. S., "Local Yielding Around a Crack Tip in Plexiglass," ASME JOURNAL OF APPLIED MECHANICS, Vol. 37, 1970, pp. 409–415.

3 Theocaris, P. S., and Gdoutos, E. E., "Verification of the Validity of the Dugdale-Barenblatt Model by the Method of Caustics," Engineering Fracture Mechanics, Vol. 6, 1974, pp. 523–535.

4 Theocaris, P. S., and Gdoutos, E. E., "The Modified Dugdale-Barenblatt Model Adapted to Various Fracture Configurations in Metals," International Journal of Fracture, Vol. 10, 1974, pp. 549–564.

5 Kalthoff, J. F., Winkler, S., and Beinert, J., "Dynamics Stress-Intensity Factors for Arresting Cracks in DCB specimens," International Journal of Fracture, Vol. 12, 1976, pp. 317–319.

6 Theocaris, P. S., "Dynamic Propagation and Arrest Measurements by the Method of Caustics on Overlapping Skew-Parallel Cracks," International Journal of Solids and Structures, Vol. 14, 1978, pp. 639–653.

7 Katsamanis, F., Raftopoulos, D., and Theocaris, P. S., "Static and Dynamic Stress-Intensity Factors by the Method of Transmitted Caustics," ASME Journal of Engineering Materials and Technology, Vol. 99, 1977, pp. 105–109.

8 Goldsmith, W., and Katsamanis, F., "Fracture of Notched Polymeric Beams Due to Central Impact," Experimental Mechanics, 1979, pp. 235–244.

9 Kalthoff, J. F., Beinert, J., and Winkler, S., "Influence of Dynamic Effects on Crack Arrest," EPRI 1022-1, First Semi-Annual Progress Report, Report V9/78, Institut für Festkörpermechanik, Freiburg, Germany, Aug. 1978.

10 Rosakis, A. J., "Analysis of the Optical Method of Caustics for Dynamic Crack Propagation," Report ONR-79-1 Division of Engineering Brown University, Mar. 1979, Engineering Fracture Mechanics, Vol. 13, 1980, pp. 331–347.

11 Theocaris, P. S., and Ioakimides, N. I., "The Equations of Caustics for Crack and other Dynamic Plane Elasticity Problems," Engineering Fracture Mechanics, Vol. 12, 1979, pp. 613–615.

12 Theocaris, P. S., and Gdoutos, E. E., "Surface Topology by Caustics," Applied Optics, Vol. 15, 1976, pp. 1629–1638.

13 Dugdale, D. S., "Yielding of Steel Sheets Containing Slits," Journal of the Mechanics and Physics of Solids, Vol. 8, 1960, p. 100.

14 Barenblatt, G. F., Salganik, R. I., and Cherepanov, G. P., "On the Non-steady Motion of Cracks," Journal of Applied Mathematics and Mechanics (English translation of PMM), Vol. 26, 1962, p. 469.

15 Rosakis, A. J., and Freund, L. B., "The Effect of Crack-Tip Plasticity on the Determination of Dynamic Stress-Intensity Factors by the Optical Method of Caustics," Report N00014-78-C-0051/5, Division of Engineering, Brown University, Sept. 1980.

16 Willis, J. R., "A Comparison of the Fracture Criteria of Griffith and Barenblatt," Journal of the Mechanics and Physics of Solids, Vol. 15, 1967, p. 151.

17 Freund, L. B., and Clifton, R. J., "On the Uniqueness of Plane Elastodynamic Solutions for Running Cracks," Journal of Elasticity, Vol. 4 1974, pp. 293–299.

18 Rice, J. R., "Mathematical Analysis in the Mechanics of Fracture," Fracture, Vol. II, ed., Liebowitz, H., Academic Press, New York, 1968, p. 191.

19 Beinert, J., and Kalthoff, J. F., "Experimental Determination of Dynamic Stress-Intensity Factors by the Methods of Shadow Patterns," for publication in Mechanics of Fracture, Vol. VII, ed., Sih, G. C., Noordhoff International Publishing, Leyden, The Netherlands.